

Inelastic second-order analysis of steel columns under minor-axis bending

<http://dx.doi.org/10.1590/0370-44672018720046>

Gilney Afonso Gonçalves^{1,2}

<https://orcid.org/0000-0002-6663-8889>

Ricardo Azoubel da Mota Silveira^{1,3}

<https://orcid.org/0000-0001-8955-0356>

Andréa Regina Dias da Silva^{1,4}

<https://orcid.org/0000-0001-7841-8077>

Jéssica Lorrany Silva^{1,5}

<https://orcid.org/0000-0001-8525-3098>

¹Universidade Federal de Ouro Preto – UFOP, Escola de Minas, Departamento de Engenharia Civil, Ouro Preto – Minas Gerias - Brasil.

E-mails: ²gilneyafonso@gmail.com,

³ramsilveira@yahoo.com.br, ricardo@em.ufop.br,

⁴andreadiassilva@yahoo.com.br,

⁵jessicalorrany05@hotmail.com

Abstract

The inelastic second-order behavior of steel structural columns under minor-axis bending is presented in this article. To study this behavior, a nonlinear frame element formulation is adopted in which the steel's plasticity process is accompanied at the nodal points of each finite element through the refined plastic-hinge method (RPHM). A tangent modulus approach is employed in order to consider the stiffness degradation in function of the internal forces' variation, and the second-order effects, residual stresses and geometric imperfections are considered in the modeling of column behavior. As a criterium for defining the ultimate limit state of the column cross-section, strength surfaces are adopted. These surfaces describe the interaction between the axial force and bending moment (N-M interaction diagrams). To solve the nonlinear equilibrium equation for the structural system, the Newton-Raphson method is used, coupled with continuation strategies. Columns with different slenderness, boundary and loading conditions are analyzed, and the results obtained are comparable to those found by other researchers. The results lead to the conclusion that the numerical approach adopted in this study can be used for a better behavioral understanding of the steel column under weak-axis bending.

Keywords: Steel columns, inelastic second-order analysis, minor-axis bending, finite element method, refined plastic-hinge method.

1. Introduction

Nowadays, steel material is commonly employed in civil construction. Besides being a completely recyclable material, steel has important characteristics such as strength and durability, good ductility and speedy manufacturing and assembly times. For the steel member and frame structure analysis, highlighted herein is an advanced analysis that has the capacity to simultaneously evaluate its strength and stability.

In a nonlinear finite element context for steel member and frame numerical analysis, two inelastic analysis approaches are usually employed: the plastic zone

method (PZM) and the refined plastic-hinge method (RPHM). In the PZM (Clarke, 1994; Alvarenga, 2010), the cross-section of each finite element is discretized in fibers and the second order effects and residual stresses can be directly considered in the analysis. Another important characteristic is that with the stress state obtained in each fiber, it is possible to monitor the gradual yielding in the cross-section. Due to the efficiency of this method, its solutions are usually treated as "exact solutions" in literature (Chen and Kim, 1997). However, the PZM is not routinely used in engineer-

ing offices, since it requires an intense computational effort. Because of this, its application is usually restricted to the simulation of simple structures that serve as comparisons and/or calibrations for the development of other numerical models and formulations.

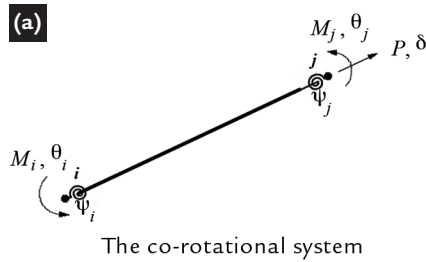
In the RPHM (Liew *et al.*, 1993; Chan and Chui, 2000), the consideration of material plasticity is concentrated at the nodal points of each finite element. At these nodes, the formation of plastic hinges can occur, characterizing the plasticity of the entire cross-section. This method is computationally more practical

and captures, in an approximating manner, the advance of the plasticity in the element cross-sections before the formation of the plastic hinges. Residual stresses effects can also be considered.

The objective of this study is to use an RPHM that permits adequate modeling for the inelastic behavior of steel columns with type I compact sections under weak or minor-axis bending. Although unusual, the columns where the bending occurs under this axis can present important benefits such as the capacity to develop all of their plastic strength without lateral-torsional buckling (BS 5950, 2000; AISC, 2005). Besides this,

2. Inelastic formulation based on rphm

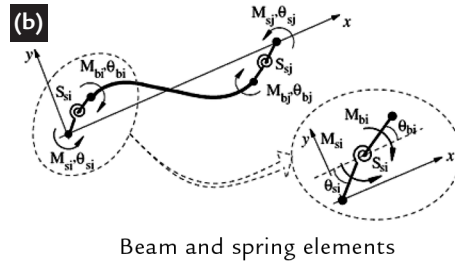
In this section, the inelastic formulation based on the RPHM implemented in CS-ASA is presented along with the main interventions made for this study. The following assumptions are considered in the column modeling: all finite elements are initially straight and prismatic and their cross-sections



for profiles having wide flanges, the shape factor is approximately 35% greater than the referent for the major axis (Kanchana-lai and Lu, 1979).

To achieve the proposed objective, the tangent modulus equation suggested by Ziemian and McGuire (2002) is implemented in the CS ASA (*Computational System for Advanced Structural Analysis*; Silva, 2009). In this equation, the cross-section stiffness degradation varies in function of the axial force and bending moment around the minor axis. The numerical formulation proposed also employs the strength surfaces (McGuire *et al.*, 2000; BS 5950, 2000), adequately

remain plane after a deformation, the steel profiles are compact, rigid body large displacements and rotations are permitted, and the shear deformation effects are ignored. The finite element utilized is the frame element delimited by nodal points i and j, with fictitious springs at the ends, as illustrated in



evaluating the interaction between the axial force and bending moment at the minor axis. Validation of these strategies is made by analysis of the columns under various boundaries, slenderness and loading conditions. The results obtained are compared with analytical and numerical solutions obtained using the PZM. In this study, the second order effects are simulated, and the nonlinear solution methodology is based on the Newton-Raphson method coupled with continuation strategies. The details of this methodology are presented on the next two sections. Section 4 presents three numerical examples.

Fig. 1a in the co-rotational system (Belytschko and Galum, 1979). Also in Fig. 1a, P, M_i, M_j and $\delta, \theta_i, \theta_j$ are the internal forces and natural displacements in the co-rotational system, respectively; the spring parameter ψ_i (or ψ_j) is associated with the plastic level of the node i (or j) and is detailed below.

Figure 1
Finite element adopted for the modelling of columns.

The objective of the RPHM is to capture the advance of the plastification at the nodal points of elements, from the beginning of the yielding to its total plastification with the plastic hinge formation. To achieve this goal, the inelastic formulation adopted in this study is based on the

proposal made by Chan and Chui (2000), where it is considered that the plasticity development in the structural members is simulated through fictitious springs (Fig. 1b). To monitor the stiffness degradation of the cross-section at the element nodal points, the parameter ψ is used,

$$S_s = \frac{6EI}{L} \frac{\psi}{1-\psi}, \text{ with } \psi = \frac{|M_{pr} - M|}{|M_{pr} - M| + |M - M_{er}|} \text{ and } M = (f_y - f_r - P/A) W \quad (1)$$

where E is the elasticity modulus, I is the moment of inertia and L is the length of the frame element; M_{er} is the bending moment when yield begins and M_{pr} is the reduced

bending moment when plasticity occurs, defined according to the choice of strength surface (see Section 3); f_y is the yield stress, f_r is the residual stress, A is the cross-section

area and W is the section elastic modulus.

In Fig. 1b, the flexural equilibrium conditions in the spring elements are expressed by equations:

$$\begin{Bmatrix} \Delta M_{si} \\ \Delta M_{bi} \end{Bmatrix} = \begin{bmatrix} S_{si} & -S_{si} \\ -S_{si} & S_{si} \end{bmatrix} \begin{Bmatrix} \Delta \theta_{si} \\ \Delta \theta_{bi} \end{Bmatrix} \text{ and } \begin{Bmatrix} \Delta M_{sj} \\ \Delta M_{bj} \end{Bmatrix} = \begin{bmatrix} S_{sj} & -S_{sj} \\ -S_{sj} & S_{sj} \end{bmatrix} \begin{Bmatrix} \Delta \theta_{sj} \\ \Delta \theta_{bj} \end{Bmatrix} \quad (2)$$

where $\Delta M_s, \Delta \theta_s$ and $\Delta M_b, \Delta \theta_b$ are the bending moments and rotation increments in the joints of the spring element

with the global node and with the beam element, respectively.

For the internal beam element (Fig.

1b), the moment-rotation relationship is given by:

$$\begin{Bmatrix} \Delta M_{bi} \\ \Delta M_{bj} \end{Bmatrix} = \begin{bmatrix} k_{ij} & k_{jj} \\ k_{ji} & k_{jj} \end{bmatrix} \begin{Bmatrix} \Delta \theta_{bi} \\ \Delta \theta_{bj} \end{Bmatrix} \quad (3)$$

where ΔM_{bi} , ΔM_{bj} , $\Delta \theta_{bi}$ and $\Delta \theta_{bj}$ are the bending moments and rotation increments associated with the nodal points

i and j of the beam element. The terms k_{ij} , k_{ji} , k_{ji} and k_{jj} are responsible for simulating the bending stiffness and second-

order effects. They are defined as (Yang and Kuo, 1994):

$$k_{ii} = k_{jj} = \frac{4E_t I}{L} + \frac{2PL}{15} \quad \text{and} \quad k_{ij} = k_{ji} = \frac{2E_t I}{L} - \frac{PL}{30} \quad (4)$$

with E_t representing the tangent modulus and L the element length.

Associating the Eqs. (2) and (3), one can arrive in the following matrix equation:

$$\begin{Bmatrix} \Delta M_{si} \\ \Delta M_{bi} \\ \Delta M_{bj} \\ \Delta M_{sj} \end{Bmatrix} = \begin{bmatrix} S_{si} & -S_{si} & 0 & 0 \\ -S_{si} & -S_{si} & +k_{ij} & k_{ij} \\ 0 & k_{ji} & S_{sj} + k_{jj} & -S_{sj} \\ 0 & 0 & -S_{sj} & S_{sj} \end{bmatrix} \begin{Bmatrix} \Delta \theta_{si} \\ \Delta \theta_{bi} \\ \Delta \theta_{bj} \\ \Delta \theta_{sj} \end{Bmatrix} \quad (5)$$

Now, assuming that the loads are applied only in the global nodes of the element (ΔM_{bi} and ΔM_{bj} are

equal to zero), making some matrices algebraic manipulations and including the axial effect (frame element),

one can arrive in the following force-displacement relationship in the element co-rotational system:

$$\begin{Bmatrix} \Delta P \\ \Delta M_{si} \\ \Delta M_{sj} \end{Bmatrix} = \begin{bmatrix} EA/L & 0 & 0 \\ 0 & S_{si} - S_{si}^2(k_{ij} + S_{sj})/\beta & (S_{si} S_{sj} k_{ij})/\beta \\ 0 & (S_{si} S_{sj} k_{ij})/\beta & S_{sj} - S_{sj}^2(k_{ij} + S_{si})/\beta \end{bmatrix} \begin{Bmatrix} \Delta \delta \\ \Delta \theta_{si} \\ \Delta \theta_{sj} \end{Bmatrix} \quad \text{or, } \Delta \mathbf{f}_c = \mathbf{K}_c \Delta \mathbf{u}_c \quad (6)$$

with $\beta = (S_{si} + k_{ii})(S_{sj} + k_{jj}) - k_{ij}k_{ji}$. The subscript c indicates the coordinate system utilized; A is the cross-section area; ΔP is the increment of axial force and $\Delta \delta$

is the increment of axial deformation. The tangent modulus E_t captures, in an approximate manner, the reduction of the element's sectional stiffness

due to the axial force. The strength equations for the columns of AISC (2005) define the variation of the tangent modulus as:

$$\frac{E_t}{E} = 1.0 \quad \text{for } P \leq 0.39P_y \quad \text{and} \quad \frac{E_t}{E} = -2.7243 \frac{P}{P_y} \ln\left(\frac{P}{P_y}\right) \quad \text{for } P > 0.39P_y \quad (7)$$

where E is the material modulus of elasticity, P is the active axial force, and P_y is the axial yield force. These equations include the effect of the

initial imperfections as well as the residual stresses in the columns. However, this is only valid for axial forces of compression ($P < 0$). For axial

tension forces ($P > 0$), the strength equations for columns proposed by CRC (Galambos, 1998) can be used and are given by:

$$\frac{E_t}{E} = 1.0 \quad \text{for } P \leq 0.5P_y \quad \text{and} \quad \frac{E_t}{E} = \frac{4P}{P_y} \left(1 - \frac{P}{P_y}\right) \quad \text{for } P > 0.5P_y \quad (8)$$

where the residual stresses effects are implicitly considered.

Ziemian and McGuire (2002) pro-

posed a modification to the equations presented in the CRC (Galambos, 1998) in which the tangent modulus varies in

function of the axial force and the bending moment about the weakest axis. In this case:

$$E_t = \tau E, \quad \text{with, } \tau = \min\left(1.0, (1+2p) \left[1 - (p + \beta m_y)\right]\right), \quad p = \max\left(P/P_y, (0.5 - \beta m_y)/2\right) \quad \text{and} \quad m_y = \frac{M_y}{M_{py}} \quad (9)$$

where the term β is an empirical value, which, in the inelastic second-order analysis, is equal to 0.65 for members

under minor-axis bending (Ziemian and McGuire, 2002); M_y and M_{py} are the bending moment and the plastic bending

moment, both in relation to the minor axis. Using these equations in the analysis of structural members under minor-axis

bending, Ziemian and McGuire (2002) obtained results that were compatible with

those encountered when using the PZM. Considering only the axial forces, Fig. 2

displays a comparison between the above Eqs. (7), (8) and (9).

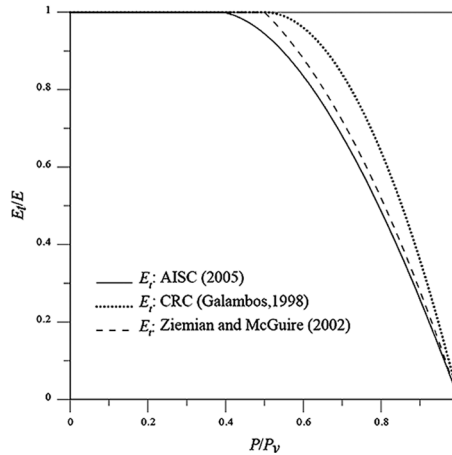


Figure 2
Tangent modulus variations.

To reach the proposed objective herein, the tangent modulus equations are utilized as indicated by Ziemian and

McGuire (2002), which depend on the axial force and moment under minor-axis bending. Since this moment is evaluated

at the i and j ends of the finite element (Fig. 1), the tangent modulus can be calculated as:

$$E_t(x) = \left[\left(1 - \frac{x}{L}\right) E_{t,i} + E_{t,j} \frac{x}{L} \right] \quad (10)$$

with $E_{t,i}$ and $E_{t,j}$ representing the modified tangent modulus at the i and j element ends, respectively.

The terms k of the stiffness matrix in Eq. (6) are recalculated taking to consideration that the tangent modulus varies linearly along the length of the finite element. Using

the appropriate interpolation functions, the first part of k_{ii} , k_{ij} , k_{ji} and k_{jj} are redefined considering E_t , through the relationships:

$$k_{ii}^* = \int_0^L \left[\frac{2}{L} \left(2 - 3\frac{x}{L}\right) \right]^2 E_t(x) I dx; \quad (11a)$$

$$k_{ij}^* = k_{ji}^* = \int_0^L \left[\frac{2}{L} \left(2 - 3\frac{x}{L}\right) \right] \left[\frac{2}{L} \left(1 - 3\frac{x}{L}\right) \right] E_t(x) I dx \quad (11b)$$

$$k_{jj}^* = \int_0^L \left[\frac{2}{L} \left(1 - 3\frac{x}{L}\right) \right]^2 E_t(x) I dx \quad (11c)$$

Resolving the previous integrals, the coefficients k_{ii} , k_{ij} , k_{ji} and k_{jj} become:

$$k_{ii} = \frac{(3E_{t,i} + E_{t,j})I}{L} + \frac{2PL}{15}; \quad (12a)$$

$$k_{ij} = k_{ji} = \frac{(E_{t,i} + E_{t,j})I}{L} - \frac{PL}{30}; \quad (12b)$$

$$k_{jj} = \frac{(E_{t,i} + 3E_{t,j})I}{L} + \frac{2PL}{15} \quad (12c)$$

Equation (6) is valid until the internal forces reach the section plastic strength. From then on, with the section having already suffered total plastification, the increase of the axial force, for

example, creates a condition where the strength of the section is less than that of the forces acting upon it. As such, an alteration in the force-displacement relationship is necessary so that the

strength plastic equations for the section are not violated. This alteration and the transformation of Eq. (6) into the global coordinates system is detailed in Gonçalves (2013) and Silva (2009).

3. Strength surfaces

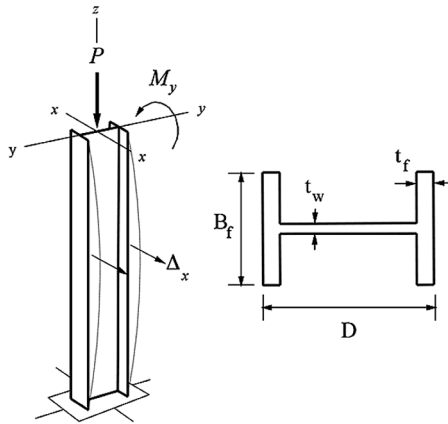
In an inelastic analysis, it is necessary to accurately estimate the ultimate capacity of the structural members. To achieve this, criteria are established that define the plastic strength limit of the structural member. Amongst the various existing criteria (von Mises, Tresca, etc.) defined from the stress state, the surface strength in which the plastic limit is reached can be determined through the

combination of internal forces in the cross-section (Orbison *et al.*, 1982; Duan and Chen, 1990). In the RPHM context, these surfaces are responsible for defining the instant in which the plastic hinge occurs (cross-section total plastification). For this study, two strength surfaces are adopted where the interaction between axial force and the bending moment in the transversal sections are evaluated.

The behavior of the structural member when the bending moment acts on the weakest axis is illustrated in Fig. 3, where Δ_x indicates the deformation due to the load applied to provoke bending.

The first strength surface, proposed by McGuire *et al.* (2000), is valid for standard American profiles of light to medium weight and can be expressed by:

Figure 3
Structural column under minor-axis bending.



$$M_{pry} = M_{py} \sqrt{(-3p^6 + \sqrt{9p^{12} - 4(p^2 - 1)})} / 2 \tag{13}$$

where M_{pry} is the reduced plastic moment and M_{py} is the plastic moment, both in relation to the minor axis. In this equation, p is the relationship between the

active axial force and the axial yield force ($p = P/P_y$).

The British Standard BS 5950 (2000) supplies expressions for the re-

duced plastic moment (M_{pr}) for compact I or H profiles in the presence of axial force. In relation to the minor axis bending, these equations are given by:

$$M_{pry} = f_y \left[Z_y - \frac{A^2}{4D} \left(\frac{P}{P_y} \right)^2 \right] \text{ for } \frac{P}{P_y} \leq \frac{t_w D}{A} \tag{14a}$$

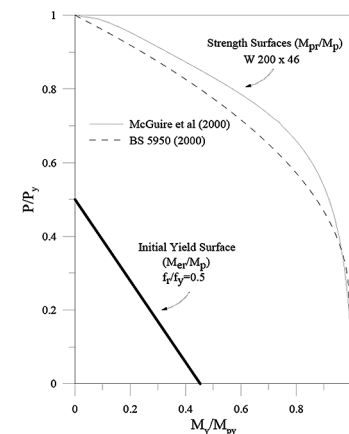
$$M_{pry} = f_y \left[\left(\frac{A^2}{8t_f} \right) \left(\frac{4B_f t_f}{A} - 1 \right) + \frac{P}{P_y} \right] \left(1 - \frac{P}{P_y} \right) \text{ for } \frac{P}{P_y} > \frac{t_w D}{A} \tag{14b}$$

where, as illustrated in Fig. 3, t_w is the web thickness, t_f is the flange thickness, B_f is the flange width, D is the height of

the profile's section and A is the area of the profile's section. The term Z_y is the minor-axis plastic section modulus.

Figure 4 illustrates the two strength surfaces obtained by the equations previously presented.

Figure 4
Initial yield and strength surfaces adopted.

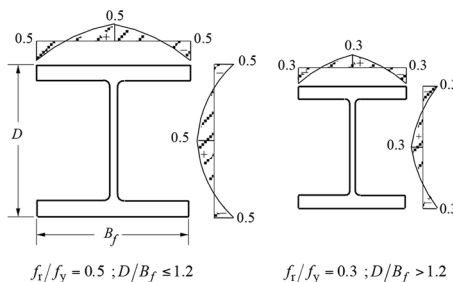


Initial yield and strength surfaces adopted

The effects caused by residual stresses are considered in an implicit manner on the tangent modulus. However, these stresses are expressed in an explicit form to determinate the bending

moment when yield begins (Eq. 1) and to obtain the initial yield surface (Fig. 4). In the present article, these stresses were defined following standard recommendations (ECCS, 1983; AISC, 2005;

see Fig. 5). It is worth mentioning that in members under weak-axis bending, the effect of residual stresses is more pronounced, since they affect the extreme fibers more.



Residual stresses as recommended by ECCS (1983)

Figure 5
Residual stresses as recommended by ECCS (1983).

4. Numerical examples

In this section, the adopted numerical strategies for the inelastic second-order analysis of columns under minor-axis bending are evaluated. Specifically, the importance of considering the modified tangent modulus model proposed by Ziemian and McGuire (2002) to simulate the stiffness degradation of the cross-section will be highlighted. Also studied are the

two plastic strength surfaces that were previously described. To demonstrate this, three columns with different load and boundary conditions are studied and the results compared with those found in literature. As nonlinear solver strategy, the generalized displacement strategy (load-increment strategy) and the minimum norm of residual displacement strategy

with the Newton-Raphson method (iterative strategy) are adopted (Silva, 2009). A tolerance factor of 10^{-4} is used.

To facilitate the presentation of the results, a simplified notation is used, given in Table 1, to refer to the different tangent modulus models. As indicated, the use of the constant modulus of elasticity is also possible.

Notation	Description: Equation
E_{t0}	Constant value
E_{t1}	AISC (2005) and CRC (Galambos, 1998): Eqs. (7) and (8)
E_{t2}	CRC (Galambos, 1998): Eq. (8)
E_{t3}	Ziemian and McGuire (2002): Eq. (9)

Table 1
Tangent modulus notation.

4.1 Fixed-Free column

Consider a fixed-free column submitted to a permanent vertical load P and a variable horizontal load H applied perpendicular to the minor axis as illustrated in Fig. 6. This example was previously analyzed by Zubydan (2011) to validate his numerical

formulations. This figure also includes the member material and geometry data, as well as the finite element discretization.

formulations. This figure also includes the member material and geometry data, as well as the finite element discretization.

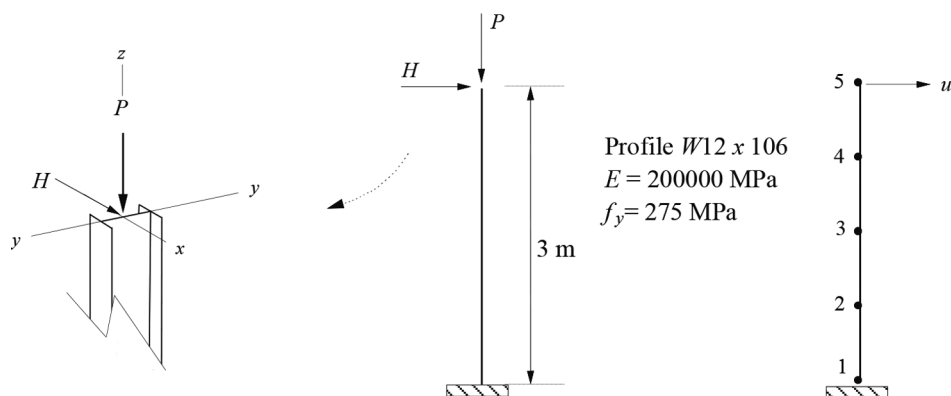


Figure 6
Fixed-free column and the finite element discretization.

The behavior of the column is investigated taking into consideration three permanent load P levels: 20%, 40% and 60% of the axial yield load, P_y . By controlling the horizontal displacement u at the top of the column, the equilibrium paths illustrated in Fig. 7 are obtained.

The values obtained for the horizontal load at collapse are summarized in Table 2.

The results obtained by Zubydan (2011), who utilized the PZM, are used for comparison. The residual stresses are defined according to recommendations

from ECCS (1983). The strength surfaces proposed by McGuire *et al.* (2000) are chosen, and the results are presented varying the representative model for the tangent modulus.

By analyzing the load-displacement curves and the collapse loads in Table 2,

it is possible to conclude that the tangent modulus E_{t3} is more efficient in forecasting the load limit. The other models overestimate the collapse load limit, especially

for high values in the P/P_y relationship.

Now, maintaining the tangent modulus E_{t3} , another analysis involving the variation of the strength surfaces is

performed. Figure 8 displays the equilibrium paths obtained. Notice the good agreement between the two strength surfaces studied.

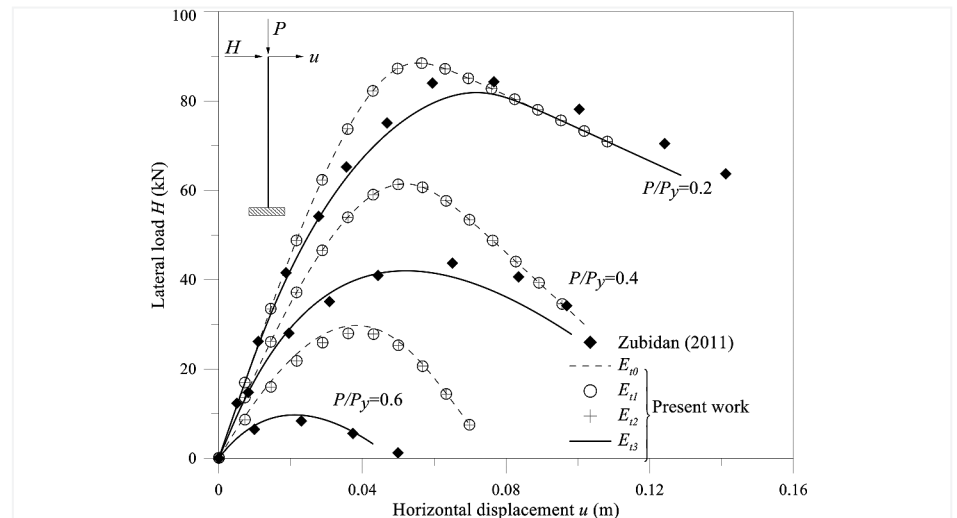


Figure 7
Free-fixed column equilibrium paths.

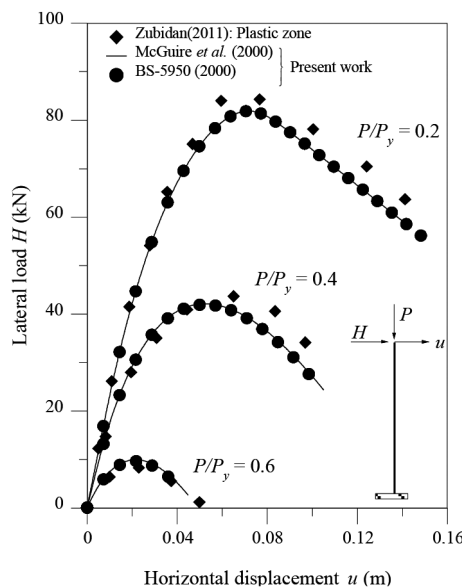


Figure 8
Equilibrium paths for different strength surfaces.

Tangent modulus	Collapse load H (kN)		
	$P/P_y = 0.2$	$P/P_y = 0.4$	$P/P_y = 0.6$
E_{t0}	88.50	61.44	29.72
E_{t1}	88.50	61.44	28.18
E_{t2}	88.50	61.44	28.18
E_{t3}	81.88	41.97	9.69

Table 2
Horizontal collapse load H.

4.2 Pinned column

Assuming that there is a permanent axial load P acting at the ends of the pinned column, two loading conditions are evaluated: the variable bending moment acting at the two ends and the variable horizontal load applied to the center of the column, as shown in Fig. 9. The column bending in both loading cases occurs under the weak-axis.

Ten finite elements are used in the

discretization of the member. The cross-section and the material data used are also presented in Fig. 9. In the analysis, the strength surface used is that which is recommended in BS 5950 and the residual stresses indicated in ECCS (1983) are adopted.

The interaction curves (axial force x bending moment) for each of these investigated columns are presented in Fig. 10. The study was made taking into

consideration the slenderness parameter L/r_y (where L is the column length and r_y the radius of gyration) equal to 40, 80 and 120. The analyses adopted E_{t1} and E_{t3} for the tangent modulus. With the finality of validating results, analytical solutions developed by Kanchanalai and Lu (1979) were employed. For the case of the column with moments at the two ends, the results obtained by Zubidan (2011) are also used.

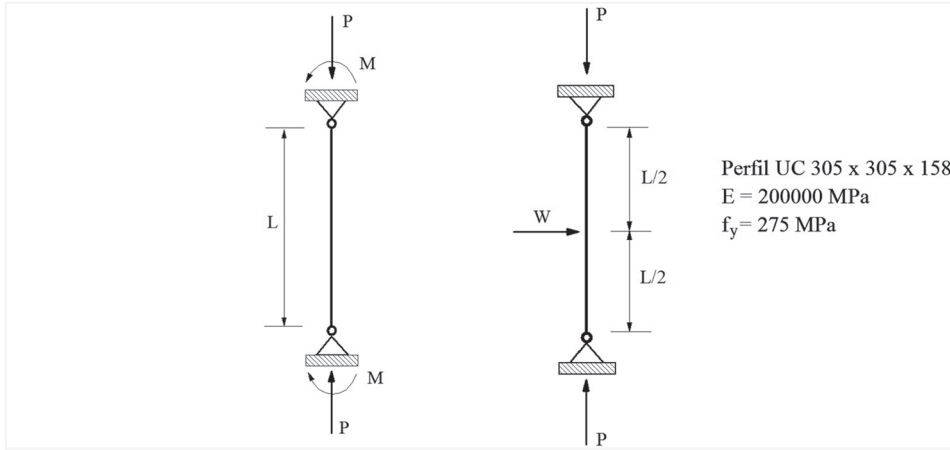


Figure 9
Pinned column under different loading conditions.

It is observed in Fig. 10a that when $L/r_y = 120$ is used with the E_{t1} tangent modulus, the interaction curve obtained is almost coincident with the analytical solution. However, for less slender parameters, the strength for

the column is overestimated. In turn, the tangent modulus E_{t3} furnished conservative curves for all of the situations related to the analytical solutions, and it is more precise when compared to the solutions by Zubidan (2011), who used

the PZM. This is also verified with the column under a horizontal load, as can be seen in Fig. 10b. In this case, with E_{t1} , good results are also obtained when $L/r_y = 40$; however, for $L/r_y = 80$, the strength is still overestimated.

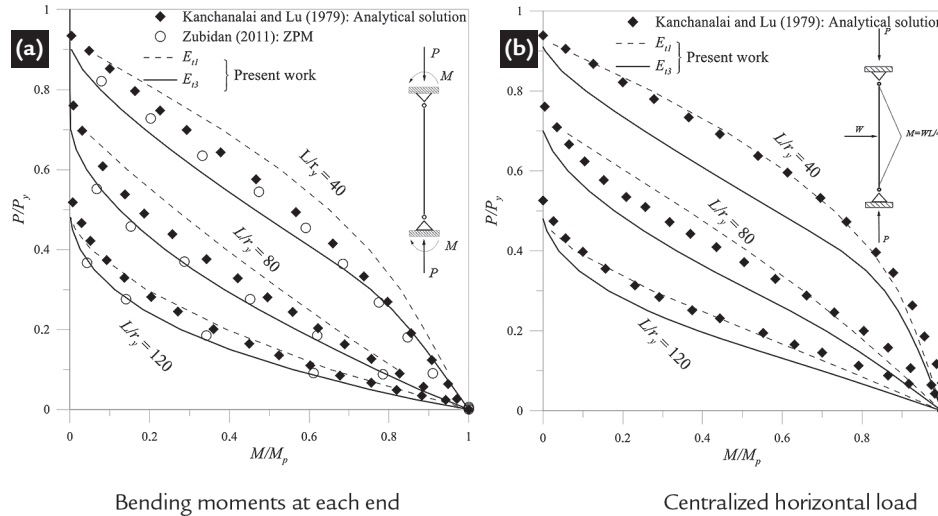


Figure 10
Pinned column interaction curves.

4.3 Pinned column with initial curvature

The last column studied is a pinned column with an initial curvature, as presented in Fig. 11. Its physical and geometrical properties, as well as the load applied on the column, are also presented in Fig. 11. It is assumed

that the initial imperfection is a sinusoidal function of $L/1000$ amplitude in the direction of the minor axis.

The column discretization is made with four finite elements. The study was done by altering the column

length so that the slenderness parameter of the column $L/(r_y \pi)(f_y/E)0.5$ varied from 0 to 2.5, approximately. The column's load limit was obtained for each situation and its variation with the slenderness index is illustrated in

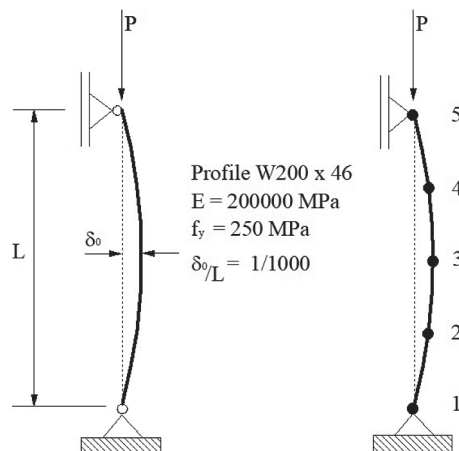


Figure 11
Pinned column with initial curvature and its finite element discretization.

Fig. 12a. A residual stress of 30%fy was adopted and the strength surface was taken from BS 5950 (2000). The results were validated when compared with those by Ziemian and McGuire (2002), who used the NIFA computational program with the PZM.

Once again, observing the results shown in Fig. 12a, the tangent modulus E_{t3} proposed by Ziemian and McGuire (2002) stands out as the best representation for the column behavior. When utilizing the modulus E_{t1} and E_{t2} , the critical load P is overestimated.

The structural response obtained using the tangent modulus E_{t3} with the strength surface suggested by McGuire et al. (2000) was also estimated. From the results presented in Fig. 12b, it is possible to conclude that when using this surface, the efficiency of modulus E_{t3} is maintained.

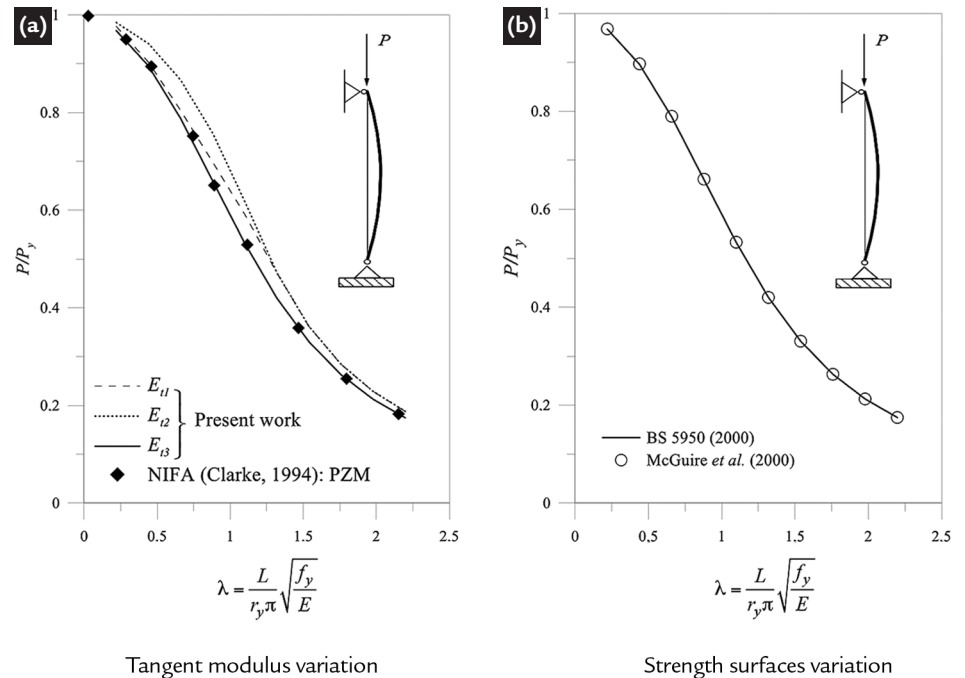


Figure 12
Pinned column:
load limit (P/P_y) x slenderness index λ .

5. Conclusions

This article presented a numerical methodology that permits the inelastic second-order analysis of steel columns under minor-axis bending. The residual stresses and geometric imperfections were also considered in the modeling of the column behavior.

The strategies adopted to best represent the steel column under minor-axis bending behavior include considering the material plasticity at the nodal points of each finite element, capturing in an approximating manner the advancement of the plasticity in the element cross-sections before the formation of the plastic hinges (RPHM), the use of appropriate strength surfaces and, mainly, the utilization of the modified tangent modulus (Eq. (9)) proposed

by Ziemian and McGuire (2002).

Based on the results obtained, it can be concluded that the use of these numerical strategies are necessary, and these were correctly implemented. This affirmation is justified, since the results obtained here generally agreed with the analytical or even numerical solutions from literature. Additionally, the good results reached with the modified tangent modulus were evident in the load-displacement curves and load-slenderness curves of the investigated columns. Better accuracy of the results compared to the analyses performed with another tangent modulus available in the computational platform CS-ASA were also observed. In general, the other tangent modulus models overes-

timated the columns' critical load. Furthermore, in the interaction curves (PM interaction diagrams), the adoption of the modified tangent modulus showed good agreement with the numerical results found in literature.

The utilization of the strength surface proposed by McGuire et al. (2000) or the interaction diagram recommended by the BS 5950 (2000), together with the modified tangent modulus proposed by Ziemian and McGuire (2002), generated almost coincidental results.

Finally, the success of the results obtained guarantee the possibility of performing a reliable and realistic numerical advanced inelastic analysis of columns under minor-axis bending.

Acknowledgments

The authors would like to thank CAPES and CNPq (Federal Research Agencies), FAPEMIG (Minas Gerais State Research Agency) and UFOP/

PROPP for the financial support received. Special thanks to Professor Péter Z. Berke from Université libre de Bruxelles (ULB) for his hospitality during the

manuscript's review at Batir/ULB. They also acknowledge Prof. Harriet Reis and PaperTrue for the English review of this text.

References

- AISC. Specification for Structural Steel Buildings. American Institute of Steel Construction. Chicago, 2005.
- ALVARENGA, A. R. *As ligações semirrígidas na análise avançada com zona plástica de portais planos de aço*. Ouro Preto: Programa de Pós-Graduação em Engenharia Civil, DECIV/Escola de Minas/UFOP, 2010. 481p. (Tese de Doutorado).
- BS 5950. Structural Use of Steelwork in Buildings — Part 1: Code of practice for design — Rolled and welded sections. London, England: British Standards Institution, 2000.
- BELYTSCHKO, T., GALUM, L. Application of high order corotational stretch theories to nonlinear finite element analysis. *Computers and Structures*, v. 10, p. 175–182, 1979.
- CHAN, S. L., CHUI, P. P. T. *Non-linear static and cyclic analysis of steel frames with semi-rigid connections*. Oxford: Elsevier, 2000. p. 336.
- CHEN, W. F., KIM, S. E. *LRFD steel design using advanced analysis*. Boca Raton, Florida: CRC Press, 1997. p. 467.
- CLARKE, M. J. Plastic zone analysis of frames. In: CHEN, W. F., TOMA S. (Eds.). *Advanced analysis of steel frames: theory, software, and applications*. Boca Raton: CRC Press, 1994. p. 259–319.
- DUAN, L., CHEN, W. F. A yield surface equation for doubly symmetrical sections. *Engineering Structures*, v. 12, p.114-119, 1990.
- ECCS. Ultimate limit state calculation of sway frames with rigid joints. In: EUROPEAN CONVENTION FOR CONSTRUCTIONAL STEELWORK, 1983. 20p. (Pub. n. 33).
- GALAMBOS, T. V. *Guide to stability design criteria for metal structures*. New York: John Wiley & Sons, 1998, v. 5, p. 911. (Structural Stability Research Council).
- GONÇALVES, G. A. *Modelagem do comportamento inelástico de estruturas de aço: membros sob flexão em torno do eixo de menor inércia*. Ouro Preto: Programa de Pós-Graduação em Engenharia Civil, DECIV/Escola de Minas/UFOP, 2013. 90p. (Dissertação de Mestrado).
- KANCHANALAI, T., LU, L. W. Analysis and design of framed columns under minor axis bending. *Engineering Journal, AISC*, v. 16, n. 2, Second Quarter, p. 29–41, 1979.
- LIEW, J. Y. R., WHITE, D. W., CHEN, W. F. Second-order refined plastic hinge analysis for frame design: part 1. *Journal of Structural Division*, v. 119, n. 11, p. 3196–3216, 1993a.
- LIEW, J. Y. R., WHITE, D. W., CHEN, W. F. Second-order refined plastic hinge analysis for frame design: part 2. *Journal of Structural Division*, v. 119, n. 11, p. 3217–3237, 1993b.
- MCGUIRE, W., GALLAGHER, R. H., ZIEMIAN, R. D. *Matrix Structural Analysis*. (2nd.). New York: Wiley, 2000. 460p.
- ORBISON, J. G., MCGUIRE W., ABEL, J. F. Yield surface applications in nonlinear steel frame analysis. *Computer Methods in Applied Mechanics and Engineering*, v. 33, p. 557–573, 1982.
- SILVA, A. R. D. *Sistema computacional para a análise avançada estática e dinâmica de estruturas metálicas*. Ouro Preto: Programa de Pós-Graduação em Engenharia Civil, DECIV/Escola de Minas/UFOP, 2009. 322p. (Tese de Doutorado).
- YANG, Y. B., KUO, S. B. *Theory & analysis of nonlinear framed structures*. Prentice Hall, 1994. 579 p.
- ZIEMIAN, R. D., MCGUIRE, W. Modified tangent modulus approach, a contribution to plastic hinge analysis. *Journal of Structural Engineering, ASCE*, v. 128, n. 10, p. 1301–1307, 2002.
- ZUBYDAN, H. A. Inelastic second order analysis of steel frame elements flexed about minor axis. *Engineering Structures*, v. 33, p. 1240–1250, 2011.

Received: 26 March 2018 - Accepted: 23 April 2019.



All content of the journal, except where identified, is licensed under a Creative Commons attribution-type BY.